Miniaturization of a Water-Jet Drill for Microfracture Surgery

By D.W. Wabeke
Department of Biomechanical Engineering, Delft University of Technology

Miniaturization of a Water-Jet Drill for Microfracture Surgery

By Daan W. Wabeke

in partial fulfilment of the requirements for the degree of

Master of Science
in Mechanical Engineering

at the Delft University of Technology,
to be defended publicly on Wednesday October 11, 2017 at 10:00 AM.

Supervisor:	Ir. S. den Dunnen,	TU Delft
Thesis committee:	Prof. dr. J. Dankelman,	TU Delft
	Dr. ir G. Elsinga,	TU Delft

Table of Contents

Abstract

As part of a larger project called "Healing Water" this thesis project investigated aspects of minimally invasive water-jet drilling as a technology to be used in micro-fracture surgery. Drilling prototypes were developed and tested to gain a better understanding of the potential and the behaviour of high-pressure water jets in conjunction with minimally invasive devices. Specifically, this thesis focussed on the possible negative effects of inner diameter and curvature on drilling success.
This thesis found that minimally invasive water jet drilling (in perspex, simulating bone) is possible. However, unwanted movement due to thrust reaction is a point of concern. Dealing with the thrust reaction as well as investigating real-world practicalities and limitations of the surgical procedure should be the focus of further R&D.

1: Introduction

"Healing Water" is a research project at TU Delft into the potential uses of high-pressure water-jets in medical applications. Water-jet drilling is a relatively new field in the world of medicine. It could provide benefits such as the avoidance of heat and mechanical damage. The technique is becoming more common in various surgical disciplines such as dermatology, plastic surgery, dental surgery and orthopedics.

This thesis builds on earlier work done within the scope of the Healing Water project. The work done by Steven den Dunnen, Gabrielle Tuijthof and others [1-4] had shown the possibilities of using water-jets to drill in bone. The goal of the project was to take steps towards developing a water-jet device, suitable for minimally invasive microfracture surgery. Microfracture surgery is a technique that uses bone marrow to stimulate cartilage repair.

In the next chapter of this thesis, a detailed description is given of a pilot study into the feasibility of a flexible, minimally invasive water-jet device, capable of drilling in Perspex as substitute for bone. This study was performed as a means of reconnaissance into the complications of developing a minimally invasive water-jet drill.

Then, in chapter 3, three prototypes were developed and tested as an investigation into the possible negative effect of minimalized inner diameters and flow curvatures on the drilling capabilities of a water-jet. This chapter is structured as a stand-alone scientific article.

Lastly, chapter 4 discusses a main concern encountered in chapter 3, which is unwanted movements due to the thrust reaction and proposes some possible methods for combating this issue.

2. Minimally Invasive Water-Jet Drilling, A Pilot Study

2.1 Introduction

In the current practice of minimally invasive, microfracture surgery, the operating surface is no larger than a few square centimetres and several holes, no larger than 2 mm, need to be drilled a couple of millimetres apart and up to 4 mm deep [5]. If this is not done correctly it could impair healing and the recovery time of the patient can increase considerably.

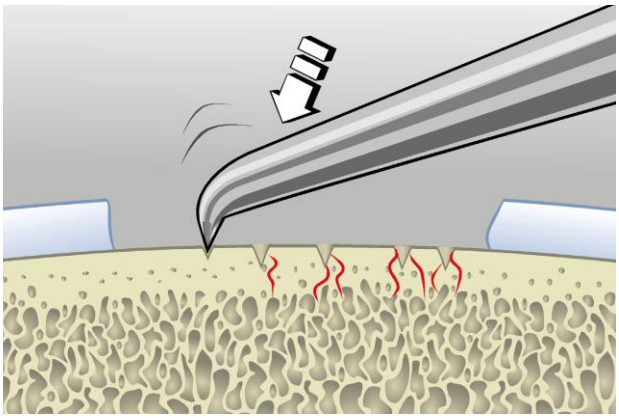

Figure 1: Orthoscopic awl penetrating subchondral bone [5]

The current procedure (typically within a joint, like a knee) often consists of hammering holes with the help of an orthoscopic awl. An example of such a device can be seen in Fig.1. This method is not very accurate and can encounter problems when accessing difficult locations and creating correctly defined channels in the subchondral plate [6]. Errors made with this procedure can damage the healthy surrounding tissue, for instance when the awl overshoots its target. Another method is using mechanical drills. Although these can be designed with a certain level of flexibility to provide the required access, they present other complications. Mechanical drilling creates heat which in turn can damage the surrounding tissue and impair the healing process [7]. Mechanical tools are also susceptible to wear during usage.

Previous research [2] has shown that a coherent water-jet at pressures of up to 70 MPa can penetrate cortical bone, perhaps obviating the need to drill or hammer by mechanical means. The jet needs to be coherent, in order to transfer power to the operating surface [8]. The research mentioned used a fixed set-up with rigid components, which can neither be considered ‘minimally invasive’ nor ‘flexible’. Consequently, the question posed was whether water-jet drilling would be possible with a device designed for flexible, minimally invasive access. This meant using flexible tubing, with a coherent water-jet exiting perpendicular to the flow direction in the tube, and with none of the elements larger than roughly 1 cm (as was considered to qualify as ‘minimally invasive’). No such device exists on the current market. The goal of this pilot study was therefore to design, fabricate and test a device along these specifications. The first experiments were designed to see if the prototype could produce a coherent jet of up to 70 MPa water pressure.

2.2 Materials and Methods

2.2.1 Prototype

The pilot prototype was developed at TU Delft and can be seen in Fig.2. The production of this prototype is detailed in appendix A. It consists of an aramid fibre braid flexible tube with an inner diameter of 1.35 mm, built to convey high-pressure fluids. A custom-made fitting consisting of an insert and a tube head connect it to the nozzle head. Tensile tests showed that an insert of this length should be able to resist a tensile force (in the direction of fluid flow through the tube) of up to 150 N. The expectation was that the design should be able to resist the force of the water hitting the nozzle head and not allow the insert to be pushed out of the tube. The nozzle head holds the nozzle with the 0.4 mm orifice that creates the drilling jet. The nozzle head was 3-D printed and designed to redirect the fluid flow so that the jet would exit the nozzle orifice perpendicular to the tube flow, onto the operating surface. (Although the outside dimensions of the nozzle head and nozzle do exceed the 10mm used as approximate limit to qualify for 'minimally invasive' surgery, these could have been trimmed to suit. However, as the focus of the experiments was primarily on the flexibility of the device, its inner diameters and the orthogonal exit of the jet, these components were not machined more than strictly necessary, for reasons of fabrication and safety)

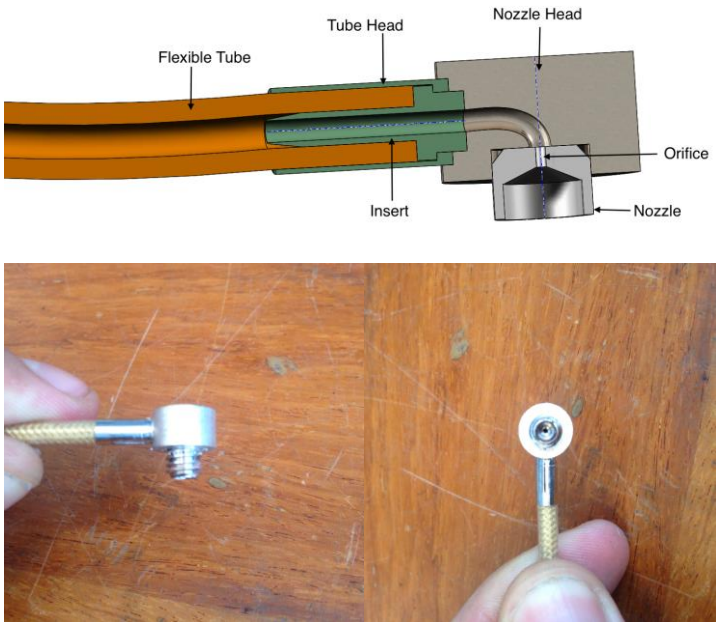

Figure 2: Pilot prototype

2.2.2 Experiments

The tests were done by creating water pressure with a hydraulic pressure bench (UTM) at TU Delft.
A set-up was created where the prototype was fixed above the work piece. This was done to absorb the expected thrust reaction of the water-jet. (See Fig.3) The work piece was a small plate of Perspex, used to simulate cortical bone. The experiments were filmed using a Go Pro camera and the pressure was measured using a pressure sensor, positioned just before the tube. During initial testing, it became clear that the splash of water from the work piece made it impossible to get a clear view of the jet coherence. Therefore, it was decided to do the initial testing for coherence by jetting straight into the water basin. Before testing the system ran a series of warm-ups in order to clear the system of air and to ensure that the setup ran smoothly. The pressure delivered by the UTM was slowly increased, starting at 1.22 MPa for safety reasons and then increasing in small steps while monitoring the jet and the device. Each time the pressure was increased from zero to the chosen maximum in 5 seconds.

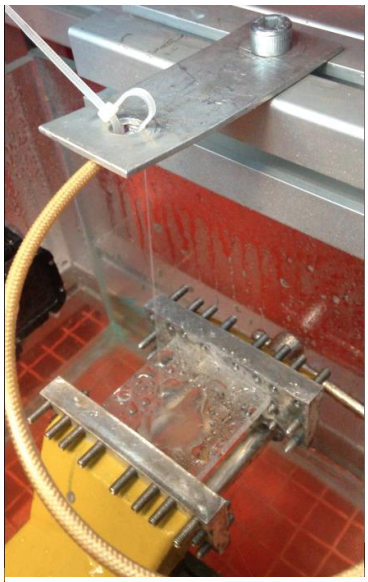

Figure 3: Experimental setup, tap-pressure jet

2.3 Results

The tested jet pressures ran from 1.2 MPa to 11.5 MPa. (Their corresponding input forces are listed in table 1.)

5 kN	10 kN	20 kN	40 kN	50 kN
1.22 MPa	2.43 MPa	4.84 MPa	9.59 MPa	11.49 MPa

Table 1: Input forces (UTM) and corresponding jet pressures in the tubing

No tests were performed beyond 11.49 MPa as the prototype ruptured at this point. The resulting jets are shown in Fig.4-8.

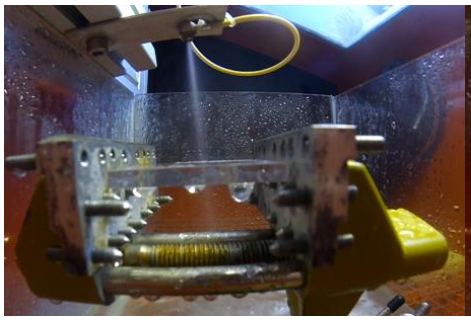

Figure 4: Jetting at 1.22 MPa

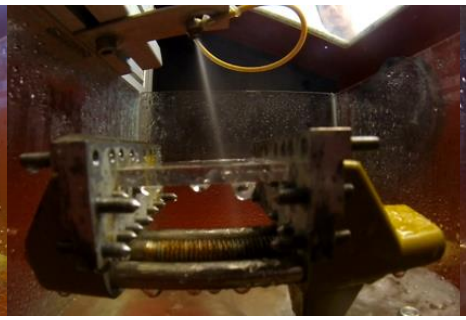

Figure 5: Jetting at 2.43 MPa

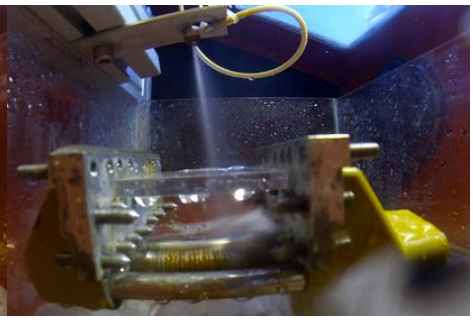

Figure 6: Jetting at 4.84 MPa

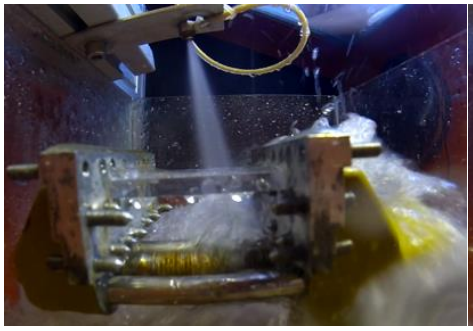

Figure 7: Jetting at 9.59 MPa

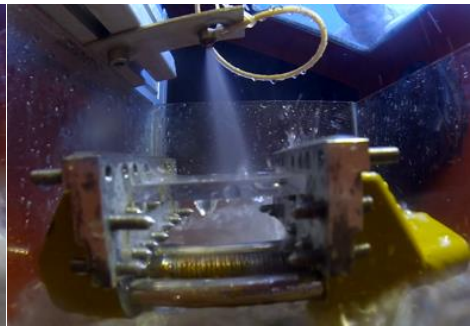

Figure 8: Jetting at 11.49 MPa

2.4 Discussion

When the jet pressure exceeded 4.8 MPa the jet started to lose coherence and became no longer suitable for drilling. The required precision could not be achieved with such a jet and the power transfer would be far too inefficient. Increasing the pressure further was not possible as the prototype ruptured at 11.5 MPa. Video recordings of the test show that the tube head slipped off the tube. Though this was regrettable the test had clearly shown that this configuration would not be able to produce a jet with sufficient power density to drill through cortical bone. In the following sections jet coherence and the rupture of the device will be discussed in detail.

2.4.1 Jet Coherence

To assess the conditions of the fluid flow (flow velocity, Reynolds value) some estimations were made. If water is assumed to be 15°C, which has a density of ρ = 1000 kg/m^3 and dynamic viscosity $\mu = 1.16 \times 10^{-3}$, the kinematic viscosity $\nu = \frac{\mu}{\rho}$ is 1.16×10^{-6}. The variables used in the calculations are:

- Water temperature: $15°C$
- Water density: ρ = 1000 kg/m^3
- Dynamic viscosity: $\mu = 1.16 \times 10^{-3}$
- Kinematic viscosity: $\nu = \frac{\mu}{\rho} = 1.16 \times 10^{-6}$
- Diameters: $D_{tube} = 1.35\ mm$, $D_{nozzlehead} = 1.1\ mm$, $D_{nozzle} = 0.4\ mm$
- Pressure: P = 70 MPa

First to find the flow velocity of the jet, a simplification of Bernoulli's equation is used:

$$V = \sqrt{\frac{2P}{\rho}} = 374.17\ m/s \qquad (1)$$

Based on this velocity the volumetric flow rate would be

$$Q = \frac{\pi}{4} D^2 V = 4.28 \times 10^{-4}\ m^3/s \qquad (2)$$

This would lead to a flow velocity within the tube of 32.85 m/s.
The formula for the Reynolds value for a smooth, straight tube, with a similar fluid flow is:

$$Re = \frac{\rho V D}{\mu} = \frac{V D}{\nu} = 3.823 \times 10^4 \qquad (3)$$

Figure 9: Previous experiment, coherent jet

The Reynolds value at the transition of laminar to turbulent flow is somewhere between 2000 and 4000, depending on the smoothness of the entry conditions. It is obvious that the flow in the tube when drilling will always be turbulent. Using these estimations as a reference we look at the different possible factors in creating a coherent jet.

The main goal of the prototype was to determine if it was possible to produce a coherent drilling jet in a flexible, minimally invasive setup. The test quickly showed that this was not the case. Looking at the images and video's it is clear that the jet has completely lost coherence at 9.5 MPa. It was not determined at what pressure exactly the jet starts to lose coherence but it is somewhere in the 5-9 MPa range. This is so far removed from a jet that would be able to drill through cortical bone (expected at minimum, around roughly 30 MPa)

that the conclusion has to be that this prototype failed in its task. Fig.9 shows an example of a coherent jet at 70 MPa. This was produced using the non-minimalized setup in previous research [3]. For achieving a coherent jet in a flexible, minimally invasive setup, the following issues could be a factor:

- The tube (2.4.1.1)
- The nozzle head bend (2.4.1.2)
- Surface friction in the nozzle head (2.4.1.3)
- Production of the assembly (2.4.1.5)
- The nozzle (2.4.1.6)

These will be discussed in detail below.

2.4.1.1 Tube

Three aspects of the tube could factor into disturbing the jet coherence. First there are the dimensions of the tube. The diameter and length may have an influence on coherence. Shortening the tube and enlarging its diameter would perhaps increase the stability of the jet (Eq.3). However, due to the intended application of the device (minimally invasive surgery) the changes that can be made in this regard are minimal and it is doubtful that they would have a significant impact.

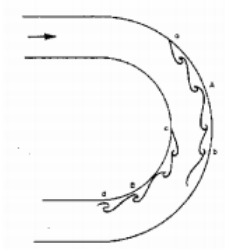

Figure 10: Flow through a bend [9]

The second aspect is the curvature of the tube. As can be seen in Fig.4-8 the flexible tube is curved in order to position the nozzle. Flow through curved tubes is a well-known phenomenon [9] and the curvature of the tube may have an effect on the flow. The difference with previous experimental setups is that in those the water flowed through a straight, large diameter pipe before arriving at the nozzle. The ability of the tube to curve in order to position the nozzle is an important and necessary feature of the device. The necessary curvature of the device would differ per procedure.
The third possible factor is the tube's flexibility, necessary to create the curvature needed to reach certain positions in a joint. The tube is susceptible to vibrations caused by the force produced by the high-pressure flow. This may also have an influence on the flow.

2.4.1.2 Nozzle head bend

The curvature of the bend is needed to direct the jet towards the operational surface. Taking into account the surgical procedure it is preferable to have the jet exit perpendicular to the flow direction at the end of the tube. Due to the requirements for minimally invasive access, the nozzle is located directly after the curvature. The hypothesis is that the flow is thoroughly disturbed in the bend and cannot develop correctly before the nozzle.
As mentioned above and shown in Fig.11 and Fig.12 the curvature causes disturbances in the flow. The water does not have an even velocity/pressure distribution across its cross-section [8]. In Fig.12 an illustration is given of the difference against mean velocity of various areas of fluid flow through a bend. As illustrated here, flow needs

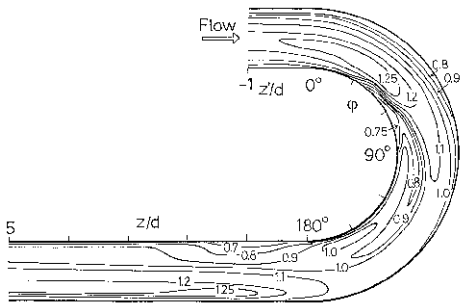

Figure 11: Mean velocity distribution in flow through curvature [8]

some distance to redevelop a uniform velocity. As the nozzle is right after the bend (Fig.2) that distance may not be available in this device. The bend just before the nozzle is also a significant difference from previous experiments, during which coherence was achieved. This bend could severely influence the jet coherence.

2.4.1.3 Surface Friction

As can be seen in Fig.12 the outer surface of the nozzle head is rough and so is the inside. With 3D printing the object is created by heating grains and the surface smoothness is therefore dependent on the grain size. This is likely to have had a negative influence on jet coherence [10].

2.4.1.4 Production of the assembly

Of concern in the production process is the correct alignment of the insert, nozzle head and nozzle. The dimensions have a certain margin and were assembled manually. Because of the size of these parts, a small misalignment could have a large impact. It was difficult to determine if this had an effect on the jet and the way to conclude this would be to build multiple similar prototypes.

2.4.1.5 The Nozzle

This is a standard sapphire nozzle, bought from Salomon Jetting Parts. It is designed to be able to handle a water pressure of up to 125 MPa and is primarily used for cleaning purposes. It consists of a stainless-steel body with a sapphire insert. These nozzles are designed specifically for creating a coherent jet and can do so with turbulent flow. Earlier experiments have shown that this nozzle was indeed able to create a drilling jet when used in a fixed, rigid drilling setup (Fig.9).
Finally, a remote possibility is damage to the sapphire prior to testing. The nozzle had been in storage for some time and was, during production of the prototype, exposed to heat from the welding process (the weld is shown in Fig.10) and to an electrical current during cleaning. However, damage of the orifice seems unlikely, as there had been no direct contact with the sapphire.

Figure 12: Connection of tube head (left) and nozzle head (right)

2.4.2 Rupture

The tube head shot from the tube when a peak pressure of 11.49 MPa was measured just before entering the tube. As can be seen in Fig.3-8, the device was held by a tie-wrap around the tube head: fixing it in place in a vertical direction. The assembly was not restricted in the horizontal direction as it was assumed the clamping of tube head to tube would hold up to larger pressures than would be encountered. Ignoring the minimal pressure drop over the length of the tube, we can calculate that a tensile force of at most 16.44 N was applied on the tube head of the prototype (Eq.1).

$$F = P * A = 11.486e10^{6} * 1.43e10^{-6} = 16.44 \text{ N} \qquad (4)$$

Here P is the water pressure in Pa, A the inner cross-sectional surface area of the tube in m^2 and F is the force in N. As water was actually flowing the actual force on the nozzle head would be lower. Examining the tube after the device ruptured it was observed that the outer PVC coating, onto which the tube head is clamped, had elongated and become significantly longer than the fibre braid. The force, applied by the fluid flow, evidently caused the PVC outer coating to stretch, which in turn will have reduced its thickness whereupon the clamping of the tube between insert and tube head will have lost its tightness (See also Fig.2).

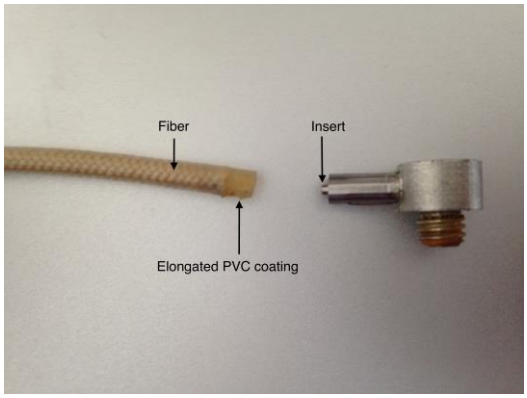

Figure 13: Prototype after rupture

There seem to be two possible causes:

- During the construction of the prototype, specifically when pressing the insert into the tube by means of a lathe, the coating may have lost its connection to the fibre braid and/or:
- The clamping was not done firmly enough. (There is no specific guideline on how much force should be applied). All the force would then need to be absorbed by the tube-head–to-outer PVC coating friction

A combination of these causes is likely, but without further testing there is still uncertainty around the root cause. However, taking the jetting results thus far into account the integrity of the device is not the most pressing issue. If a new, similar prototype were to be made the recommendation would be to first test various fittings and fitting-methods.

2.5 Recommendation

Maintaining coherence is the most important feature for any form of minimally invasive water-jet surgery to be possible. It is not known to what degree each of the factors mentioned under 2.4.1. influences the jet coherence. Further testing of these factors is required. The curvature of the bend should be a first candidate for further testing as the ability to produce a jet that can drill after this bend is of paramount importance. If this is not possible, the device loses its range of access to the operating surface.

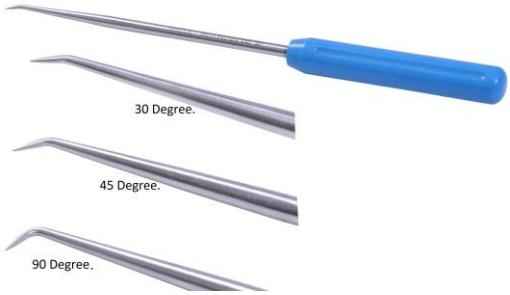

Figure 14: Orthoscopic awl

Current micro-fracture surgery uses an arthroscopic awl, shown in Fig.13. This is a straight and stiff shaft, ending in a sharp point at a certain angle. A similarly designed water-jet drill tool would have minimally invasive access, strength to withstand internal forces, stiffness to restrain movement and the benefits of a water-jet as opposed to a classic tool. Creating several versions of such a design (similar to Fig.13) could allow testing for the effects of the different degrees of curvature on jet coherence. If “an awl-jet” is not able to produce a coherent drilling-jet then it is fair to wonder if it micro-surgery using a high-pressure water jet will be at all possible. For the next prototype the design should be simplified, eliminating several possible causes for jet disturbance in order to determine the effect of just the end-curvature on jet coherence. This means minimising surface roughness, simplifying production,

eliminating flexibility and preventing possible alignment issues. All prototypes should only differ in angle of the nozzle head. The design would be based on the current orthoscopic awl. Several prototypes should be created, each with a different curvature just before the nozzle. In order to retain relevance, the dimensions should not exceed what would be acceptable to minimally invasive surgery. The goal would be to prove the mechanical possibility of drilling holes in bone-like material (perspex) with a water-jet exiting, from a small (+/- 1.35 mm) inner-diameter tube or pipe.

2.6 Conclusion

Several issues were encountered when trying to produce a drilling water-jet from a device with minimally invasive dimensions and flexibility. Though the prototype failed before the appropriate jet pressures were applied, it was clear that loss of jet coherence was the biggest concern. Given the level of complexity of the device and its production it was difficult to pinpoint the exact causes. The main differences between this device and previous experiments (that did manage to create a coherent jet) are miniaturisation and flexibility. Therefore, in order to develop a minimally invasive device for bone debridement, the exact influences of the various features of the miniaturisation and flexibility on jet behaviour need to be determined, starting with the curvature of the bend just before the nozzle orifice.

3. Miniaturization of a Water-Jet Drill

Research into the feasibility of minimally-invasive surgery with water-jet-drilling

Abstract

Water-jet drilling is a new technique for orthopedic surgery. Contrary to conventional drilling tools it does not create heat dissipation or tool wear. One intended application is the use of a water-jet for microfracture surgery, where small holes are drilled into bone in order to allow bone marrow to regenerate damaged cartilage. Previous research has proven the possibility to drill in bone using an industrial sized water-jet drill setup. For minimally invasive access to the joint space, water-jet drilling could allow a tube, fixed to a nozzle, to be used for drilling. The expectation was that the minimally invasive dimensions would increase flow turbulence and that would result in a loss of jet coherence. The loss of jet coherence could mean a decrease in power density and this would impair the jets' drilling capabilities. The effect of the minimalized inner diameter (1.4 mm) of the tube, and the sharp curvature needed to direct the jet towards the operational surface, were investigated. Three prototypes that met the minimally invasive requirements were developed for testing. These prototypes had curvatures just before their nozzle: 0, 45 and 90 degrees. The prototypes were tested for drilling success, drilling depth and coherence. Drilling was performed on a perspex workpiece at pressures ranging from 12 MPa to 70 MPa in steps of 12 MPa. All prototypes produced the same level of drilling success and reached similar drilling depths. Curvatures did not show to have a negative effect on jet coherence. The results from the experiments showed that it is possible to produce a water-jet, capable of drilling through cortical bone, using a device that meet the minimally invasive dimensional requirements for microfracture surgery.

3.1 Introduction

Microfracture surgery is a common bone debridement treatment used to treat cartilage defects by creating holes in the underlying bone in order induce bleeding to stimulate cartilage growth [5, 11]. Currently, this procedure is performed with conventional rigid tools such as a drill or an arthroscopic awl [12]. These tools can present complications during and after the procedure. Firstly, cartilage defects can be located at points in the joint space that are difficult to reach and even more difficult to operate on using stiff tools [13]. Secondly, conventional drills dissipate heat and that can lead to unwanted heat-necrosis of the surrounding tissue, which impairs to ability to heal. Water jet drilling could potentially present a new method for bone debridement treatments [2] that isn't impaired by a lack of accessibility, since water could be conveyed through flexible tubing allowing better access to hard to reach places. Additionally, its impact would not induce heat necrosis [4].
Research done by den Dunnen et al. [3, 4] shows that a water-jet is capable of drilling through subchondral bone tissue. However, in this research, an industrial size setup was used to create the water jet. This system is not suited for minimally invasive access due to its size (24 mm nozzle width), which exceeds the 10mm incision and is greater than the joint space. Commercially available products that fit the dimensional requirements for minimal

invasive water jet drilling and that are able to withstand the pressure and flow do not exist. Hence, to determine the feasibility of using pure water jets for arthroscopic bone debridement treatments, additional research is required.

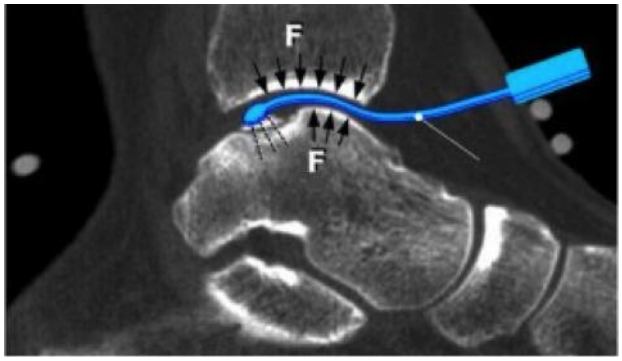

Figure 15: Flexible water-jet drilling, ankle concept

The primary challenge in developing a water jet instrument suitable for minimally invasive access is conveying the fluid flow towards the joint space and create a water jet capable of drilling in bone tissue, whilst not exceeding the dimensional restrictions for access of the joint. These requirements entail that the device can enter through an incision no larger than 10 mm [12] and can direct the jet perpendicular to the bone surface. An illustration of what is could look like is shown in Fig.15. Conveying a high-pressure fluid flow through a small, flexible tube could present complications with regards to its diminishing drilling capabilities. A pilot study with an on-scale prototype showed an incoherent water jet that was not able to drill in bone tissue. In that pilot, it was determined that the small diameter of the tube and its sharp curvature just before the nozzle were main causes of concern with regards to the jet incoherency and its ability to penetrate subchondral bone [14]. The goal of this research is to determine whether a device with minimally invasive dimensions (small inner tube diameter and a sharp curvature) can produce a water-jet capable of drilling in bone tissue. For that purpose, three prototypes with the same inner diameters and with different curvatures were developed and used to water-jet drill through bone-like tissue.

3.2 Materials and Methods

3.2.1 Theoretical Overview

The concern regarding the miniaturization of an industrial sized water-jet set-up is its potential negative influence on the capability to machine bone tissue. The reasoning is that the minimization of the dimensions of the prototype impair the fluid flow in such a manner that the prototype cannot produce a jet with a sufficient power density P_d ([W/m^2] or [kg/s^3]) [1] for drilling. Power density is the amount of power in the jet, spread out over the impact surface of the jet on the workpiece. The power density can be determined using Eq.1:

$$P_d = \frac{P_{wj}}{A_i} \quad (1)$$

Where P_{wj} is the power of the water-jet (W or [kg m^2/s^3]) and A_i is the impact surface area (m^2) of the jet. The power of the jet can be expressed with Eq.2:

$$P_{wj} = p_{wj} \cdot \dot{q}_{wj} \quad (2)$$

Here p_{wj} is the pressure (Pa or N/m^2) and $\dot{q}_{wj}$ is the volume flow rate (m^3/s) of the water jet. This volume flow rate can be expressed in Eq.3:

$$\dot{q}_{wj} = c_d \cdot A_n \cdot v_{wj} \quad (3)$$

Where c_d is the coefficient of discharge of the nozzle, A_n is the surface area of the nozzle (m^2), v_{wj} is the velocity of the water jet (m/s). The value of c_d is usually between 0.6 and 0.9 [1].

The jet must reach a sufficient power density for drilling to take place. From Eq.1 it can be determined that the jet needs to maintain a small surface area in order to maintain the power density and be able to translate that to the operational surface.

A fluid jet in an open environment diverges due to the process of mass and momentum transfer [15]. The anatomy of a high-speed water-jet in air is shown in Fig 16.

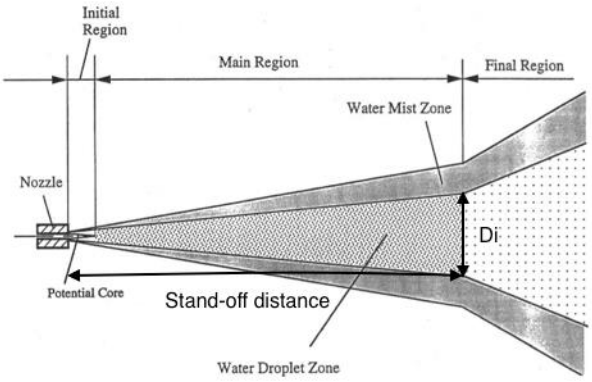

Figure 16: Anatomy of high-speed water jet in air [15], Di is the jet width at the stand-off distance, i.e. impact location

The water-droplet zone is the part of the jet that transfers the jet power to the operational surface. The power density on the operational surface diminishes as the cross-sectional area of the droplet zone increases (Eq.1) [1]. This research focusses on whether the minimally invasive dimensions before the nozzle impair the power density of the jet to the point that it is not capable of drilling.

Based on a pilot experiment with a water jet instrument that meets the dimensional restrictions of arthroscopic surgery, two main factors were identified that negatively affect the power density of the water jet: (1) the inner diameter of the tube that connects the pump to the nozzle, and (2) the change in direction of the water flow just before the water exists at the orifice, which is required to ensure perpendicular drilling in the bone tissue. Both factors will be discussed in the following paragraphs.

Inner diameter of tube

The inner tube diameter has an influence on the state of the fluid flow, which can induce turbulence of the fluid flow, causing a divergent water jet with a low power density. The level of turbulence of the fluid flow is indicated by its Reynolds number [16]. The Reynolds value is dependent on the inner tube diameter and the fluid velocity. The fluid velocity and the Reynolds number can be determined with the Eq. (4,5):

$$V = \sqrt{\frac{2P}{\rho}} \qquad (4)$$

$$Re = \frac{\rho V D}{\mu} = \frac{V D}{\nu} \qquad (5)$$

Here V is the flow velocity (m/s) in the tube, P is the water pressure (N/m^2), ρ is the fluid density (kg/m^3), D the tube diameter (m) and ν is the kinematic viscosity. The Reynolds number is indicated by Re and μ is the dynamic viscosity. The Reynolds number is the ratio of inertial forces to viscous forces and the key indicator of the flow state. Laminar flow transitions into turbulent flow when the Reynolds number exceeds the value of the boundary layer, which is approximately 4000. In a situation where microfracture surgery would be performed using a water-jet drill, the fluid will be pressurized in order to deliver the level of impact needed for ablation. For this purpose, a high fluid velocity is needed, i.e. highly pressurized flow, which results in a high Reynold number.

Change in direction of flow

Curvature changes fluid flow by turning the flow from its directional velocity, as shown in Fig.4:

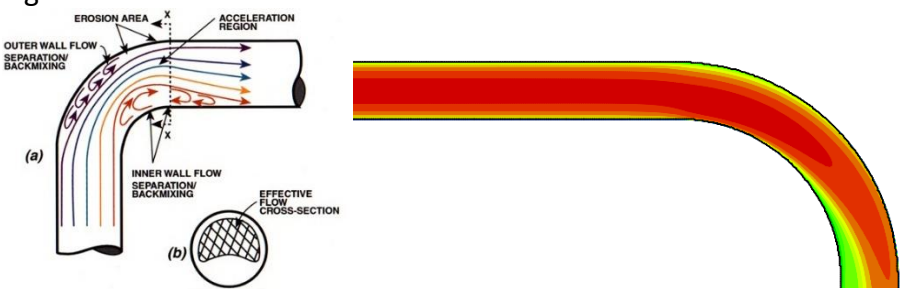

Figure 17: Fluid flow through curved pipe [17]

Fluid pressure builds up on the far side of the pipe (indicated by red in Fig. 17) and redistributes the effective flow cross-section [17]. Therefore, the flow can't fully redevelop before hitting the nozzle orifice, enhancing the turbulence of the jet exiting the nozzle and thereby diverging the water jet.
In order to be able to successfully drill in bone through minimally invasive access, it must be determined whether these dimensional requirements allow the production of a jet with a high enough power density for bone debridement. Using Eq.4, assuming an inner tube diameter of $1.4\ mm$ and water pressure $70\ MPa$, and a water density of $1000\ kg/m^3$, the flow velocity within the tube would reach an estimated $32.9\ m/s$. This would lead to a Reynolds value of $4.4 \cdot 10^5$, which is higher than the threshold of 4000 for turbulent flow. A Reynolds value of that magnitude would mean a high level of turbulence. The expectation is that an increase of turbulence in the jet will decrease the coherence [18], which diminishes the power density. The minimum power density for drilling in high density bone is approximately $1.3 \cdot 10^{10}\ \frac{W}{m^2}$ [1]. Assuming the tube flow velocity and water pressure mentioned earlier and with a nozzle diameter of $0.4\ mm$, the velocity of the water-jet is estimated to be 374 m/s. Choosing a discharge coefficient of 0.8, the volume flow rate of the jet would then be $3.76 \cdot 10^{-5}\ m^3 s$. If the jet has a water pressure of $70\ MPa$ the jet power would be an estimated $3.23 \cdot 10^4$ W. Assuming the given minimal threshold for bone drilling and using Eq.1 the impact area should not exceed $2.5\ mm^2$. When the jet is less coherent, i.e. the impact area is larger than $2.5\ mm^2$, the power density would fall below the threshold and drilling would not occur. Any possible losses due to fluid friction or other external factors were ignored in these estimations.

3.2.2 Experiment considerations

The aim of these experiments is to determine whether water-jet drilling in cortical bone is possible using a device that met minimally invasive standards. Specifically, the goal was to determine the possible negative effect of a minimalized inner diameter of the pipe on the drilling capabilities of the jet. Also, the goal was to observe whether a sharp curvature before the orifice had a negative effect on the drilling capabilities of the jet. For that purpose, three prototypes were developed that incorporated the inner diameter and curvature that would be similar to a minimally invasive surgical device. The prototypes are shown in Fig.5 and are named for their respective curvatures: P0, P45 and P90.

Figure 18: prototypes P0, P45 and P90

Prototype P0 is used as a zero measurement for the effect of curvature on jet quality. P90 has a curvature of 90 degrees and so it directs the jet perpendicular to the tube flow as could be desired for bone debridement.

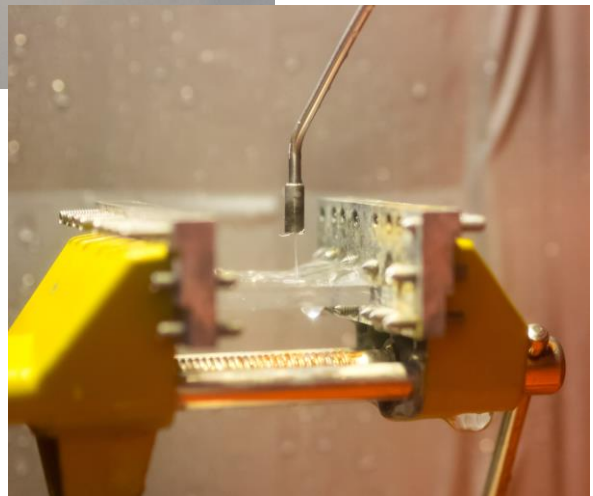

P45 was seen as a mid-way point of 45 degrees. All prototypes have 100 mm of straight piping before the final curvature. The straight piping allows flow to develop in the direction of the tube (Fig.18). The initial curvature of P45 and P90 is needed for vertical alignment of the nozzle with regards to the workpiece (Fig.19). The radius of curvature is equal for all prototypes at 7 mm. The inner diameter of the tube is 1.4 mm. It was determined in previous research by Dunnen et al. [2] that, with a nozzle orifice of $0.37\ mm$ diameter, a waterjet pressure of $70\ MPa$ was able to always penetrate any bone type, regardless of density. Therefore, the maximum pressure used for this study is 70 MPa, combined with a commercially available nozzle of 0.4 mm.
Drilling will be tested at six jet pressures, starting at 12 MPa, increasing in steps of roughly 12 MPa to 70 MPa.
The machinability of the target material (in this case cortical bone) by a liquid jet depends on material mechanical properties [19], especially the tensile strength (MPa). Perspex was chosen as a workpiece for drilling as it resembles the mechanical material properties of cortical bone, as can be seen in table 2.

Figure 19: Experimental setup, P45 at stand-off distance (10 mm) from perspex workpiece

Mechanical Properties	**Cortical Bone**	**Perspex**
Tensile Strength (MPa)	50-151	75
Compressive Strength (MPa)	100-230	124
Elastic Modulus (GPa)	7-30	3
Fracture Toughness (MPa $m^{1/2}$)	2-12	12

Table 2: Material Properties [19}

3.2.3 Experiment

Holes were water jet drilled in 5 mm think Perspex by the three prototypes using a water jet set-up previously described by Dunnen et al. [4]. Pressures were varied between 12 MPa and 70 MPa in 6 consecutive steps of 10-12 MPa (Fig.21). The water jet time was kept constant at 3 s. The prototypes were positioned perpendicularly to the drilling workpiece. The stand-off distance was kept 10 mm constant. Every water-pressure was tested 4 times in order to determine a rate of success.

3.2.4 Measurements

The pressure was monitored using a pressure sensor located just before the prototype. Hole depths in the Perspex were measured using a dial gauge. Drilling success would be defined by depths greater than 0 mm, which would indicate that the jet was capable of bone ablation. An increase in drilling depth was considered to be an increase in success.
The water jets of the prototypes were

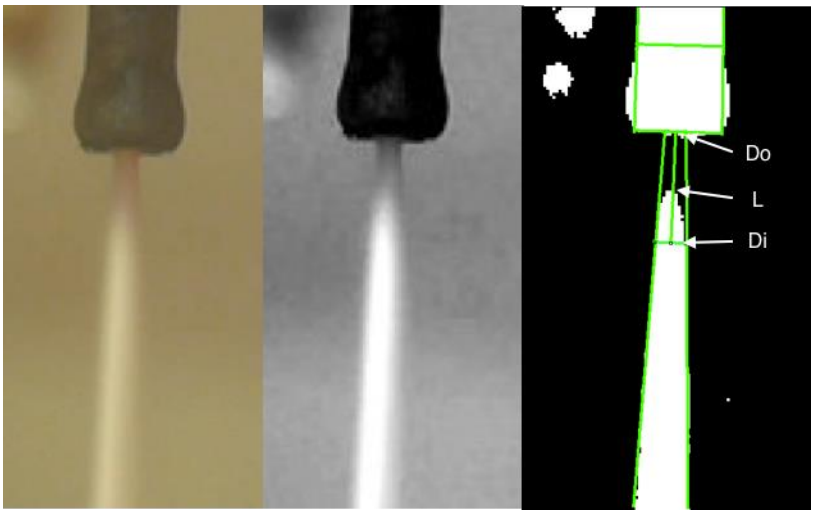

Figure 20: Coherence measurement P90, 24 MPa. Do is jet width at orifice, L is stand-off distance, Di jet width at stand-off distance

filmed in order to measure coherence, which was defined as the change in jet width, from the origin of the jet to the stand-off distance of 10 mm. Still frames were captured of the jet at drilling pressure within the first second of the 3 second jetting time. Measurements were done using ImageJ. Images were converted to 32-bit, after which the contrast were enhanced by 5% and the colour values of the pixels were normalized (white having value 1, black having value 0). Then the pixel value for the edge of the jet was determined manually and a threshold was created accordingly. The width of the jets was measured at distance 0 mm and distance 10 mm (stand-off distance) using the width of the nozzle head as reference. An example of the coherence measurement is shown in Fig. 20.

3.2.5 Statistics

In order to determine whether a prototype was successful at drilling at a certain jet pressure the ratio of success was tested for significance. The successful drilling results were tested against the total drilling iterations using a single-sample t-test [20].
These results will be compared with regards to prototype angle and water-pressure [15, 21]. Jet coherence was filmed in order to help explain potential differences in drilling success rate between the different prototypes and jet pressures and therefore not statistically tested for significance.

3.3 Results

3.3.1 Drilling Success

All three prototypes machined holes in Perspex for pressures between 24 and 70 MPa (Fig.21 and Fig.22). The single sample t-test rejected drilling success for 12 MPa and accepted drilling success for 24-70 MPa.

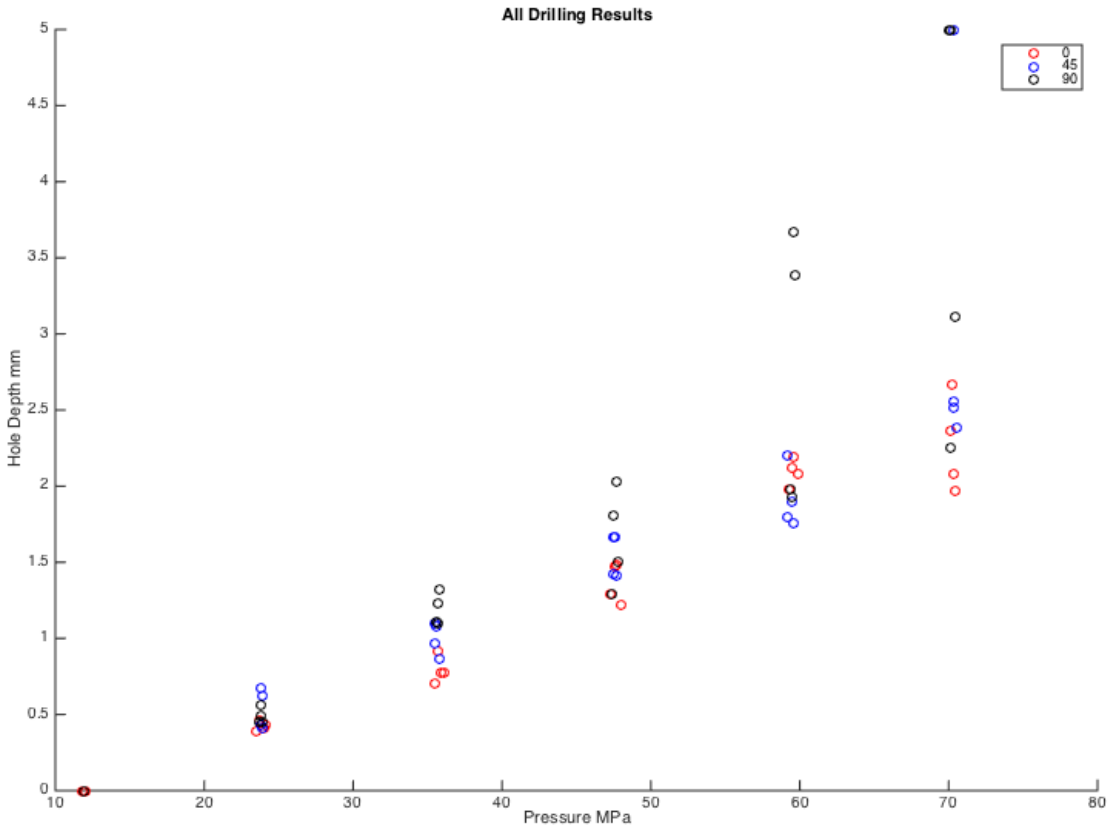

Figure 21: Drilling results, hole depth vs jet pressure

In 3 cases, the water jets fully pierced the Perspex, which are indicated by a 5mm measurement in Fig. 21. Fig.22 shows the drilling results of P45 in a work piece.

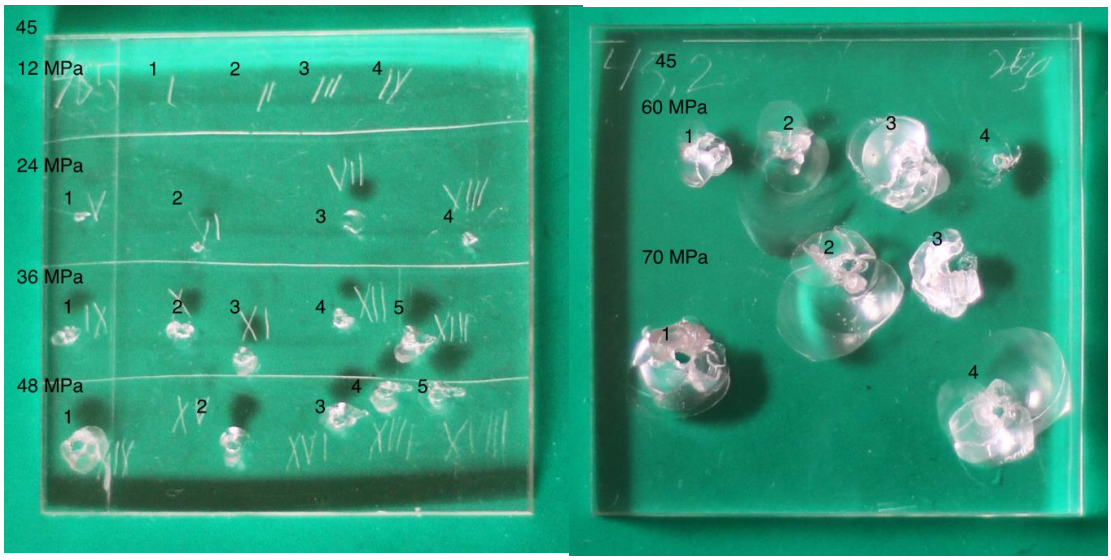

Figure 22: Drilling results, prototype 45. A fifth test was performed at 36 MPa and at 48 MPa because there was no pressure measurement at iteration 4.

3.3.2 Coherence

The change in jet width over the stand-off distance is an indication of the coherence of the jet. In table 3 the width of the jet at the stand-off distance for each prototype, at each jet pressure capable of drilling, is given (mm).

	0	**45**	**90**
24 MPa	2.0	2.0	2.1
36 MPa	2.1	2.2	2.0
48 MPa	2.0	2.5	2.0
60 MPa	2.1	2.2	2.2
70 MPa	2.1	2.2	2.1

Table 3: Jet width (mm) at stand-off distance (10 mm)

3.4 Discussion

3.4.1 Drilling Success

This study showed that a water jet instrument with minimally invasive dimensions is able to produce a water jet with a high enough power density to drill through cortical bone, using a device with minimally invasive dimensions. Observations were made by drilling in perspex with water jet prototypes that used tubing and curvatures required for arthroscopic water jet surgery. Previous tests showed that the minimum jet pressure needed for drilling success was roughly 24 MPa. This study found that all three prototypes, P0, P45 and P90, recorded drilling success at roughly 24 MPa and higher pressures. No prototype recorded drilling success at 12 MPa. The curvatures right before the nozzle did not have a negative effect on drilling success. The expectation was that prototypes with a curvature would be less successful but P45 and P90 had the same level of success as P0.

3.4.2 Drilling Depth

An increase in drilling depth was considered to be a positive development as it related to a potential microfracture surgery application. In microfracture surgery, holes need to be drilled up to 4 millimetres deep. All three prototypes achieved an increase in depth as jet pressure increased. The drilling depth increases linearly at first. As jet pressure increases, the variance in depth between iterations increases and it is no longer clear if the increase in depth is linear. All three prototypes reached roughly 2 mm, at minimum, at 70 MPa with a drilling time of 3 seconds. The minimum depth achieved is important as a device would need to be able to drill though minimally 2 mm of cortical bone before reaching weaker trabecular bone [3].

P45 drilled straight through the 5 mm perspex once at 70 MPa and P90 drilled through twice, at 70 MPa. In these cases, the jets created large fractures throughout the perspex and a crater on the exit side of the perspex. An example can be seen in Fig.8, iteration 1 at 70 MPa. What was notable was that the drilling depth reached by P0 was more consistent and P0 did not create craters in the same manner as P45 and P90. The reason for this could be that P0 did was not as susceptible to a thrust reaction as was visible with P45 and P90. It is possible that movement of the jet during drilling altered the reaction of the perspex workpiece, causing larger areas to be removed. That reaction would explain why prototypes P45 and P90 occasionally reached greater depths than P0.

3.4.3 Coherence

The tests for coherence were performed in order to help illustrate the differences in in the depth results as a more coherent jet would retain more power density then a less coherent jet and therefore should reach greater drilling depths (Eq.1). The drilling depth results showed that the prototypes were equally successful and these results were strengthened by the coherence results. The expectation was that curvature in the prototype have a negative effect on the jet coherence. The results showed no noticeable difference between the different jets produced by the prototypes.

Contrary to expectations, the jets showed no noticeable difference in coherence between the lower pressure iterations and the high-pressure iterations. In table 3 the jet width at the stand-off distance is shown. The results show a jet width of roughly 2.2 mm, regardless of prototype or jet pressure. The consistency of the jet width is important as it suggests that the nozzle is capable of preventing any effect of the curvature on the jet coherence. Therefore, a curvature before the nozzle does not negatively influence the power density of the jet and its drilling capabilities.

3.4.4 Power Density

Based on observations, the jet width at the point of impact was approximately 2 mm A diameter of 2 mm would lead to an impact area of roughly 3.1 mm^2 (πr^2), assuming the jet is symmetrical. At the maximum jet-pressure of 70 MPa the jet power would be 3.23· 10^4 W (Eq.2, Eq. 3). The jet power and the impact area would lead to an average power density of 1.03· 10^{10} W/m^2 (Eq.1), which is below the before mentioned threshold of 1.3· 10^{10} W/m^2 above which machining takes place. For this calculation, a universal distribution of the power of the jet is assumed. However, in reality, the power distribution is not uniform and this is why drilling did occur. The power density increases towards the axis of the jet and

therefore the jet can still drill [15]. The increase in power density in the middle of the jet can also be observed by the diameter of the drilled holes (roughly 1 mm).

Comparing the images of the jets produced by prototypes P0, P45 and P90 to the jets produced in previous research, this mist zone seemed far thicker. The size of the mist zone is probably due to the increased turbulence of the jets as they exited the nozzle as the jets already seemed less coherent at their base. The state of the jet could mean that there is some loss of power density when jetting through minimally invasive instruments. However, these minimally invasive devices should retain enough power density to drill and this seems to be the case.

3.4.5 Limitations

Though the material properties of perspex are very similar to cortical bone [19], it is expected that cortical bone would behave somewhat different in these circumstances. Perspex is a brittle material and high-pressure jets would sometimes blast larger pieces of perspex loose. Therefore, it was difficult to accurately compare drilling depths between prototypes. For future research, it would be recommended to use actual cortical bone as it would give a better representation of the water-jet behaviour for microfracture surgery.

A larger sample size of drilling depths might allow a better statistical comparison between prototypes but for this study, it was not considered to be too relevant as perspex would still react differently than cortical bone. Therefore, their statistical differences were not deemed as important.

Using thicker workpieces would prevent jets from drilling straight through and that would lead to more definitive results when greater depths are achieved.

For future research, it would also be necessary to improve the sturdiness of the setup, preventing vibrations, kick-back and other potential movement from having an effect on the drilling result.

For the coherence measurements, it was difficult to get an accurate, consistent measurement. In the future, video measurements could be improved by using better contrasts between the jet and its surroundings and by ensuring consistent lighting for the images.

3.4.6 Recommendations

The next step in the process of developing a water-jet based surgical tool for microfracture surgery would be to replace the stiff pipes with flexible tubing. Another step would be to harness the thrust reaction of the jet. Especially when a flexible tube is added to the device.

3.5 Conclusion

This study has shown that it is possible to successfully water-jet drill though bone, using a device with minimally invasive dimensions (inner tube diameter and sharp curvature). Experiments also showed that certain curvatures before the nozzle did not negatively influence the jet coherence or the jets drilling capabilities.

4. Thrust Reaction Prevention

4.1 Introduction

An important takeaway from the water-jet drilling experiments was the reaction of the P45 and P90 prototypes to the thrust of the jet exiting the nozzle. This phenomenon was also observed with the pilot prototype. This movement is why a main recommendation moving forward, from chapter 3, is preventing unwanted movement due to the thrust reaction of the device. For microfracture surgery, drilling precision is very important. The operational surface area is often no larger than 20 mm^2 and multiple holes need to be drilled, roughly 3-4 mm apart [5]. If the distance between holes is less than 3 mm there is a risk of creating fractures between holes. This would negatively influence the rehabilitation of the tissue. Also, movement during drilling could cause unnecessary damage to healthy tissue. This chapter introduces notional ideas on how to prevent unwanted movement due to the thrust reaction.

4.2 Observations

During the experiments in chapter 2, the nozzle head of the flexible prototype was fixated in order to prevent movement of the nozzle while jetting. Because of this fixation, the device was not susceptible to unwanted movement induced by the thrust reaction but it

was evident that a significant force acted on the device in the vertical direction due to the thrust created by the jet exiting the nozzle orifice.

During the testing of the effects of miniaturisation, in chapter 3, there was visible movement due to the thrust reaction with prototypes 45 and 90 (no movement was visible with prototype 0 as the thrust reaction force was directed along the axis of the device). Though the prototypes were made from thick walled stainless steel (AISI 304) and rigidly clamped at their inlet, some movement was observed when jetting at pressures of 36 MPa or more. Jetting at high pressures is a must in order to drill deep enough to fully penetrate cortical bone.

Absorbing, controlling or preventing the thrust reaction is therefore a crucial aspect in successfully developing a water-jet device for minimally invasive surgery.

4.3 Theoretical Background

As every action has a reaction, so has the high velocity emission of a jet by means of a nozzle [22]. Elementary momentum theory states that the resultant force acting on the control volume equals the variation rate of momentum of the liquid through the control ports. Simply put, the resultant force on the nozzle head is equal to the force of the jet exiting the nozzle. A simplified estimation of the thrust reaction can be made with the following equation [23]:

$F = \dot{m}v$ (1)

Here F is the thrust force (N), $\dot{m}$ the mass transfer and v the fluid velocity.

The mass transfer at the nozzle orifice is calculated as followed:

$\dot{m} = \rho A v$ (2)

Here ρ is the water density (kg/m^3) and A is the nozzle orifice surface area (m^2).

Assuming a water density of 1000 kg/m^3, a fluid velocity of 374 m/s, with a nozzle orifice diameter of 0.4 mm, the force on the nozzle head, in the opposite direction of the jet, would be roughly 11.26 N. These calculations give a simplified estimation of the size of the thrust reaction.

4.4 Preventing unwanted movement

Preventing the occurrence of the reaction force is not possible and therefore the objective is to absorb, control or counter it in order to prevent unwanted movement. Looking at different industries that employed water-jet technology, or just encountered circumstances that might be comparable to the circumstances of water-jet microsurgery, the distinction was made between active and passive prevention, depending on whether or not some form of energy has to actively be applied during the procedure in order to counteract the thrust force. Then several solutions were devised, not necessarily with an actual concept in mind, and categorised accordingly. This mind map is depicted in table 4:

Thrust reaction prevention			
Active:		*Passive:*	
Suction	Active suction Vacuum	**Increased stiffness**	Permanent Temporary
Counter-Jet	Stabilizing end-piece	**Adhesion**	Mechanical Chemical Electrostatic Diffusive
Magnetism	Internal External		
External tool	extra incision		

same incision	**Normal force**	Tissue Added Device
	Anchoring	Clamp Screw Mooring

Table 4: Mind-map of conceptual solutions for thrust prevention

The next step was brainstorming manners in which these mechanisms could be applied in a concept and how this would function in conjuncture with a water-jet device. Different aspects of these mechanisms were weighed for their complexity, invasiveness and overall potential. After some deliberation, the choice was made for three mechanisms that seemingly had the most promise or had compelling real-world examples from other industries.

4.5 Notional Ideas

4.5.1 Normal Force

Using a normal force to counter the thrust reaction is predicated on the fact that the operation would take place within the confined space of a joint, such as the ankle or knee. The thrust reaction is directed in the opposite direction of the jet and this would be, in most cases, in the direction of another part of bone. If the thrust reaction were to push the nozzle head upwards it could be countered by the normal force applied by the surroundings. When, as an example, microfracture surgery is performed in the patellofemoral joint, the presence of the patella could be used to an advantage. The patella is held in place by the quadriceps- and the patellar tendon, both more than capable of applying enough force to counter the thrust reaction [24]. The concept is to wedge the device in place in the designated joint, using the natural forces provided by the surrounding tendons to counter the thrust reaction. As a primary requirement of the device is that it is minimally invasive, the idea is that the means of fixation is integrated within the device and is expandable. This study looked at two basic concepts that could achieve this.

4.5.1.1 Whipstock Anchoring

This concept is based on radial jet drilling technology used in petroleum engineering. This technique uses a self-propelling water-jet drill bit to drill for oil in a horizontal direction. After drilling a well straight down into the earth the drill is lowered to the level where oil can be found and then drills radially. The device used to direct the drill and keep it at the right level is called a whipstock [25]. This technique is not all to dissimilar to water-jet based micro-fracture drilling as the drilling direction is often perpendicular to the direction of the device and the device needs to be kept in place. It is kept in place by its anchoring jaws. These extrude from the device and wedge themselves against their surroundings. An example of such a whipstock system is shown schematically in Fig.23.

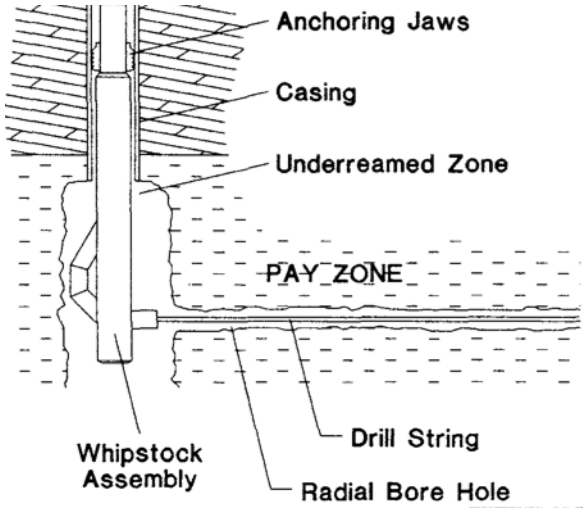

Figure 23: Whipstock assembly [25]

In this concept, the whipstock would be a case around the nozzle head that also contains the anchoring jaws. These would function similarly to the mechanism of a retractable bic-pen.

4.5.1.2 Expandable

This concept is based on the idea of expanding the drill-head in order to jam it in the correct location, using the normal forces from the surrounding joint to keep it in place during drilling. Expansion is performed after the nozzle is positioned correctly in order to allow easy access to the joint space. Expansion could be achieved in multiple ways; a spring system or inflatable bodies are some examples. Using a balloon is inspired by similar techniques used in colonoscopy [26] and angioplasty [27], where an inflatable balloon is used to keep the device in place.

4.5.2 Suction

The idea here is to include a suction cup in the design of the nozzle head. A vacuum would be created that would induce a force that can counter the reaction force generated by the jet. The suction cup would have to be designed in a way that the vacuum is not disturbed by the flow of water. In Fig. 24 is a simple depiction of the working of a suction cup. This solution has a few options when it comes to its design, mainly with regards to the suction cup design. Depending on the design, the suction cup would attach to either the opposing joint surface or the surface surrounding the operational surface.

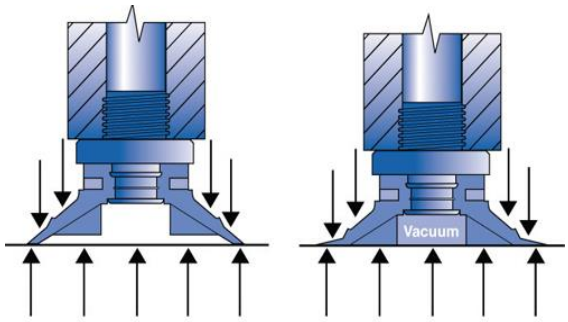

Figure 24: Suction cup

4.5.3 Counter-jet

This concept uses a jet in the opposite direction to counter the reaction force from the drill-jet. The nozzle head would in this case become a stabilizing end piece [28, 29]. The inner workings of this mechanism are explained in by Rinaldi et al. [29]. In Fig. 14 an example of a drill-bit with stabilizing end-piece is shown.

Figure 25: Drill bit with stabilizing end-piece

4.6 Discussion

The whipstock concept has the advantage of being relatively modular with regards to the surrounding joint space. This is necessary as each joint space, as well as the operating surface, presents unique circumstances. The design and manufacturing could be relatively simple and its application should be relatively straight forward. One issue with this concept is whether the anchoring jaws can be fixated securely enough, without damaging surrounding healthy tissue.

Using a balloon or springs as an expansion method for fixating the device is also relatively modular to the surrounding tissue. An issue here is that this method lacks rigidity

and there would still be some movement. Therefore, precision could still be an issue. Also, when using expanding materials there could be an issue with visibility for the surgeon.

The concept of using suction as a means of fixation has the benefit that it could quite easily be combined with other concepts. A combination of ideas could possibly solve the different drawbacks that each might have. An obvious problem that could be encountered is the effect of the water-jet on the cup's ability to maintain the vacuum. Another issue could be the necessary size of the suction cup. Lastly, the shape of the joint space and the surface area could make it impossible to successfully maintain vacuum.

A benefit of the counter-jet concept is that it is easily integrated into the nozzle head design and it would not need to significantly increase its size. Also, multiple counter-jets could be used (Fig.3) to increase stability in multiple directions and limit the damage to surrounding, healthy tissue. Another issue is the irrigation of the water-jets. Water-jet surgery would need a pump to drain the used water from the patient. More jets would demand a lot more from the pump and it is questionable whether this is possible in this setting.

4.7 Conclusion

In previous chapters the focus was on determining whether it was possible to create a minimally invasive device capable of water-jet drilling. Though this seems possible, the question is whether this could actually be applied in real-world circumstances. The first step in answering this question would be to prevent unwanted movement due to a thrust reaction. During this study, it became clear that not only is thrust prevention an important issue for developing a water-jet based surgical device, it is also an extremely complex issue. The notional ideas are very basic and should be seen as examples of what theoretically could be done. At this point, with each concept, the validity of each benefit is still doubtful and every issue is probably larger than expected. Using the naturally provided surrounding of the joint space would likely be the preferred manner in which to prevent unwanted movement. However, possible harmful effect on surrounding healthy tissue would need to be examined.

5. Conclusion

Before the pilot prototype failed, it showed a loss of jet coherence that would render drilling success impossible. The main differences between this device and those used in previous experiments (that did manage to create a coherent jet) were miniaturisation of the inner dimensions and flexibility. The pilot study concluded that the possible negative effects of device miniaturization on jet coherence needed to be investigated. The main study focussed on the inner diameter of the device and the curvature of the bend just before the nozzle orifice. The prototypes P0, P45 and P90 showed that it is possible to successfully drill though bone, using a device with minimally invasive dimensions. The results of the experiments performed with prototypes P0, P45 and P90 showed no negative correlation between curvature and jet coherence or between jet pressure and jet coherence.
The experiments conducted with all four prototypes showed that these high-pressure jets created a formidable thrust reaction that resulted in unwanted movement. This thesis investigated some notional ideas, that are very basic and should be seen as examples of what theoretically could prevent unwanted movement.

Water-jet based microfracture surgery remains a very complex issue. Though this thesis provides some early indications of its feasibility, the most complex issues are still

ahead. Though drilling with a miniaturized device is possible, but this does not mean that surgery is possible. This thesis concludes that if water-jet based microfracture surgery is to become realistic possibility, the next steps in the Healing Water project should focus on flexibility of the device and precision during drilling.

6. Acknowledgements

I would like to acknowledge the following individuals for their aid on this project:

For her guidance in the development of this thesis:
Dr. ir. G. Tuijthof Zuyd University & Academic Medical Centre

For his support in the metrology for the experiments:
J. van Driel TU Delft

For their support in the prototype development:
J. van Frankenhuyzen TU Delft
C.J. Waaijer TU Delft
R. van Antwerpen TU Delft

Appendix A: Prototype Development

The following is a detailed description of the development and production of the prototypes used for this thesis.

Pilot Prototype

The pilot prototype was developed to investigate the behaviour of a flexible water-jet drill that met minimally invasive requirements. As such a device did not exist, the prototype was designed to incorporate the necessary features for minimally invasive microfracture surgery: a flexible tube, a small inner diameter and a nozzle that can direct the jet perpendicular to the operating surface. This prototype is shown in Fig.1.
The details of the development of this prototype are given below.

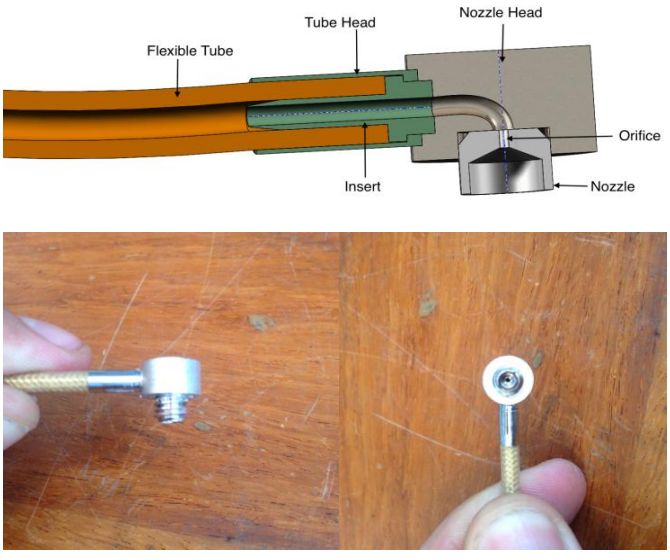

Figure 26: Pilot prototype

Nozzle

The nozzle is a sapphire nozzle with a 0.4 mm

Figure 27: Sapphire nozzle, Salomon Jetting Parts

diameter orifice from Salomon Jetting Parts. Part of the thread is shaved off to make it fit within the nozzle head, fixed by laser welding. The purpose of this nozzle is to create a coherent jet from the turbulent flow through the tube. The nozzle has a M6 housing that works for this application but would be considered too large for minimally invasive access. The housing could have been removed further but for this application there was no need to risk damaging the sapphire nozzle. This nozzle is depicted in Fig.2.

Nozzle Head

The nozzle head was designed to hold the nozzle and connect it to the tubing. It is designed to bend the fluid flow such that it exits perpendicular to the tube. The intent was to minimize disturbance and losses in energy by making the bend as smooth as possible. However, due to the small size of the device, given the need to also fit the nozzle, very little room is left for significant design benefits. Due to the complicated inner dimensions the nozzle head was 3D-printed at i.materialise, a 3D-printing company in Belgium. The nozzle head is shown in Fig.3.

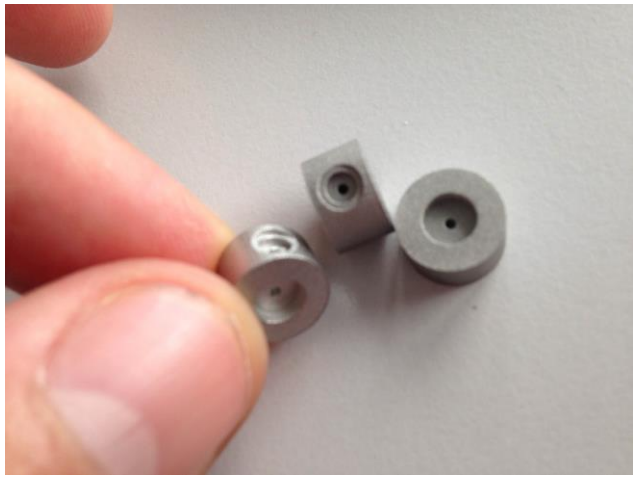

Figure 28: 3D printed nozzle head, i.materialise

Tube Head & Insert

These parts were designed to attach the tube to the nozzle head. Based on earlier tests the expectance was that this would allow up to 150 N of force. The insert was pressed into the tube using a lathe. Sealant was used to prevent possible leakage during jetting. Then the tube head was pressed on top of this and clamped on to tighten. This is shown in Figure 5. Once the tube was firmly attached to the insert and tube head this assembly was fitted into the side of the nozzle head. This opening can be seen in figure 3. Laser welding to the nozzle head fixated the tube head.

Figure 29: Tube head & insert

The start of this weld can be seen in figure 6. It is clear that the surface of the nozzle head is a lot rougher than that of the tube head. This could prove to be detrimental to the stability of the fluid flow and must be taken into account when evaluating the results.

Tube

The tube (seen in Fig.1 and Fig.5) is made by New England Catheter. It consists of a clear

Figure 30: Tube head fixated in lathe

Figure 31: Laser weld, tube head to nozzle head connection

nylon tube, aramid fibre braid and is coated with a PVC top coat. The inner diameter is 1.35 mm, the outer diameter 3.65 mm. It can withstand pressures up to 1900 bar.

P0, P45 and P90

The following gives a description of the production of prototypes P0, P45 and P90. These are depicted in Fig.7.

Figure 32: prototypes P0, P45 and P90

Pipe

These prototypes were designed to incorporate an inner diameter of 1.4 mm, similar to the flexible tube used in the previous prototype. The pipes used were stainless steel (AISI 304) and produced by Salomon's Metalen bv. The pipe's outer diameter was 3.2 mm and wall thickness 0.9 mm. The prototypes had 3 different angles before the nozzle: 0, 45 and 90 degrees. In order to create these angles a custom pipe bender had to be constructed. This pipe bender is schematically shown in Fi.8. It was designed to tightly pull the pipe over the 7.5 mm radius wheel. This radius was chosen as it was the minimal radius of curvature allowable for the pipe. A sharper radius caused kinking. On the underlying plate, markings depicted the desired angles of 45 and 90 degrees. Both P45 and P90 were curved twice for alignment purposes (see Fig.7).

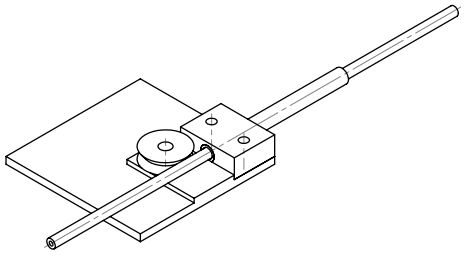

Figure 33: Custom pipe bender and pipe

Nozzle

The pipes were fitted with a nozzle head at the end. The nozzle head was simply a larger piece of aluminium with a thread on the inside to fixate the nozzle. The nozzle head was soldered onto the pipe. Then the nozzle head was fitted with an M4 sapphire nozzle form Salomon Jetting Parts. This nozzle is depicted in Fig.9.
Again, the dimension of the nozzle and nozzle head are larger than desired for minimally invasive access but suited for the purpose of this research.

Figure 34: M4 nozzle, Salomon jetting Parts

Appendix B: Experiment Protocol

Here a description of the experimental protocols and setup used for this thesis are given.

Experimental Setup

The setup used during these experiments was the same setup used in previous research [1-4]. A description of this setup is seen in Fig.1.

1. UTM
2. Red Box & Bucket

High Pressure Components:

3. Nozzle holder
4. Nozzle 3-way coupling
5. Sensor Adapter
6. Pressure sensor
7. Male-Male connecter
8. Nozzle valve
9. Nozzle hose
10. Nozzle hose swivel coupling
11. Main 3-way coupling
12. Cylinder-hose swivel coupling
13. Cylinder hose
14. Pressure release valve
15. Hydraulic cylinder
16. Male-male connector
17. Feed-water valve

Low Pressure Components:

18. Feed water hose
19. Tap water splitter
20. Sprayer hose
21. Sprayer
22. Tap water hose
23. Water faucet

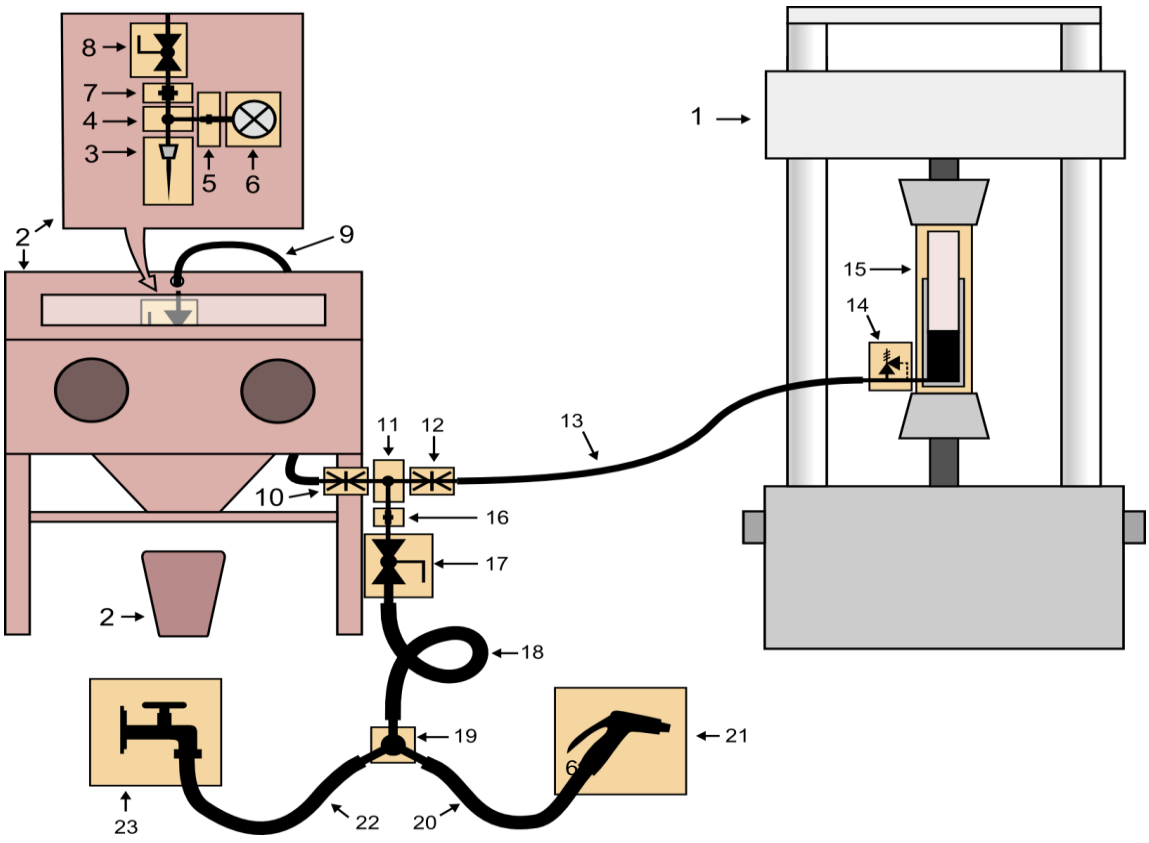

Figure 35: Experimental setup

The UTM (1) is a tensile testing machine, used at TU Delft. This machine was used to generate a force up t 295 kN. The UTM was fitted with a hydraulic cylinder (15). By applying the force generated by the UTM, the cylinder could pressurise the water up to 70 MPa. The water would be transported through a hose (13, 9) and eventually reach the prototype that was fixated in the nozzle holder (3). The prototype was aligned above the perspex workpiece

within the red box (2). Fig.3 shows the actual UTM without the hydraulic cylinder. Fig.4 and Fig. 5 show the setup of the pilot prototype and P45 respectively within the red box.

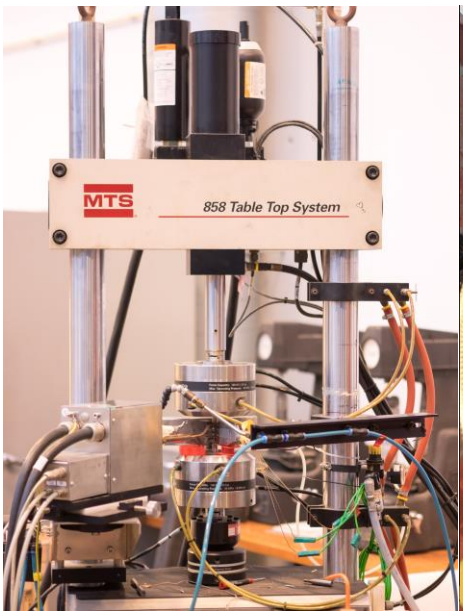

Figure 36: UTM

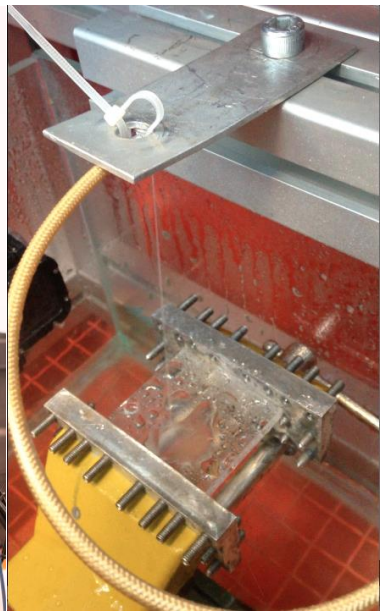

Figure 37: Pilot prototype setup within red box

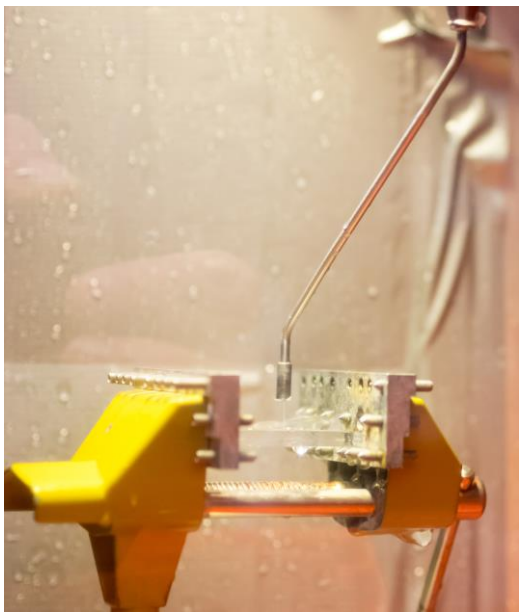

Figure 38: P45 setup within the red box

Experiment Protocol

This protocol is about water-jet experimentation with prototypes developed at TU Delft. The goal will be to drill holes in the Perspex workpiece with the water-jet produced by the prototypes. These experiments will record drilling success, drilling depth and jet coherence. The jetting will be filmed.
The protocol for assembly, operation and disassembly, used by Dunnen et al. [1-4] was used for this protocol.

Pre-testing

In order to increase the possibility of successful testing the system should be run and tested before installing a prototype. Air could get into the system and influence water-flow. Also as the system is susceptible to rust, particles could get loose in the system and block the nozzle. Therefore, the system must be run and a small range of water-pressures so any particles will be jetted out before testing commences. Pre-running the system should be at increasing pressures until no rust colour can be seen in the jet exiting the system. This is also useful for detecting possible leaks. Between prototypes the system should be run a few times again in order to dispel air bubbles and rust particles. All fittings should be made sufficiently water-proof by using Teflon-tape. This includes the nozzle and the prototype fitting. For the drilling tests, it is necessary to have a large number of identical pieces of Perspex as all tests must be done on the same workpiece. The piece of Perspex is 5 mm thick and the surface is 40 by 40 mm. A testing piece will be used for when the force is enough to damage the workpiece but not penetrate. When this is achieved a workpiece for recording is used. The workpiece is placed at a stand-off distance of 10 mm to allow the jet to form. Each iteration the force is increased quickly and reaches the limit within 0.8 seconds. This is chosen because the goal is to determine the result at that chosen peak force and therefore it is important to limit potential pre-drilling at lower forces. The gain is not quicker because of safety precautions. A separate workpiece per prototype is necessary and for every hole it must be recorded what the pressure was that was applied. For the coherence tests no workpiece is needed as the workpiece will only cause splashes and possibly interfere with the imaging. The coherence will be measured in front of an even background (flat, grey) and be measured over the stand-off distance of the previous experiments.

Drilling

It is important to gradually increase the force produced by the UTM with regards to safety. Pilot test will be done in order to determine if the setup is constructed correctly and safely and to determine if the prototype can withstand the forces produced by the high-pressure water flow. The water-pressure will be measured just before the prototype using a pressure sensor. The pressure should not differ greatly from what is to be expected with the corresponding force. Pressure losses in the system should be kept at a minimum.
At 295 kN the cylinder is expected to create roughly 70 MPa of water-pressure. At this point the jet is expected to penetrate the workpiece. The goal of the pilot tests is to determine whether the prototype can withstand these forces and at what pressure the workpiece is penetrated. When penetration is achieved, normal testing can begin.

Drilling Tests

Once penetration of the workpiece is detected the prototypes will drill 4 times, within the range between the minimally needed pressure and 70 MPa. This is done to determine the success rate of the prototype regardless of pressure. It is done 4 times in order to increase the significance of possible results. The results will be recorded in the appendix. When

switching prototypes the workpiece must also be switched. It is important to note the pressure per hole and the prototype used.

Jet Coherence

The second experiment is aimed at determining jet coherence and how this is affected by curvatures before the nozzle. The goal is to compare the coherence of the jets over the entire range of applied forces for all three prototypes. Comparing these will give insight into whether the force and the prototype shape influence the coherence. The jets will be filmed and photographed during jetting. Jet coherence will be measured by how much the jet diverges between exiting the nozzle orifice and the stand-off distance of 10 mm. After jetting the results will be measured by analyzing video and photo images of the jets. Jet coherence will be measured while jetting at the same pressures as drilling. This can't be done simultaneously as the vapor created by the drilling impact makes filming impossible. This way the relation between curvature and jet coherence can be compared as well as the relationship between coherence and jetting quality. Precautions should be taken to protect cameras from getting wet.

UTM Settings

- Maximum height: -83.5
- Minimum height: 55
- Force increase: 0.8 seconds

Testing Procedure

The experiments are performed by 2 operators. The first will control the UTM, controlling the force that is to be produced and the time over which it is reached. The second operator controls the camera and the measurement recording by the pressure sensor. This operator also controls the water flow into the system. The testing follows these steps:

- Operator 1 initiates the UTM
- Operator 2 opens the water-flow
- When the cylinder in the UTM is filled operator 2 closes the water-flow
- Operator 1 sets the UTM, sets the force, the gain speed and the fail-safes
- Operator 2 starts the pressure measurement and engages the camera
- Operator 1 engages the UTM
- When the UTM action is finished operator 2 stops the camera and the pressure sensor recording
- Operator 2 opens the water-flow (important not to allow air into the system)

When switching prototypes, it is important to clean and dry the used prototype. When testing is finished, it is important to clear, uncouple and dry all the orifices.
Prototypes P0, P45 and P90 will jet at 12 MPa, 24 MPa, 36 MPa, 48 MPa, 60 MPa and 70 MPa. The prototypes will jet 4 times at each pressure.

Appendix C: Experimental Results

Drilling Success

The tests for drilling success were done on 5 mm thick pieces of perspex. Every prototype drilled at 6 different water pressures: 12 MPa, 24 MPa, 36 MPa, 48 MPa, 60 MPa and 70 MPa. All performed 4 iterations of every pressure on the perspex workpiece. The results can be seen in Fig.1-3.

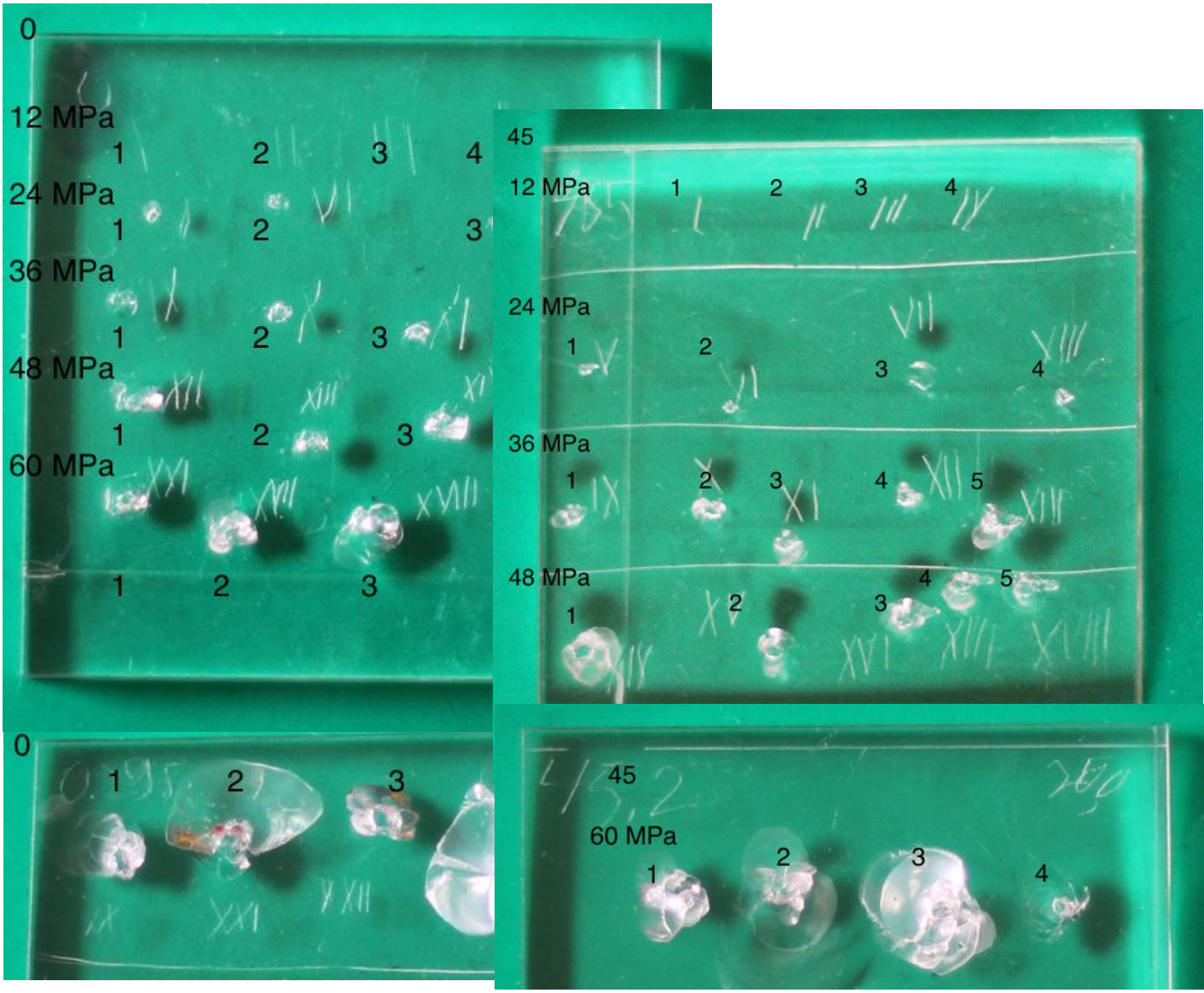

Figure 39: Drilling results, P0

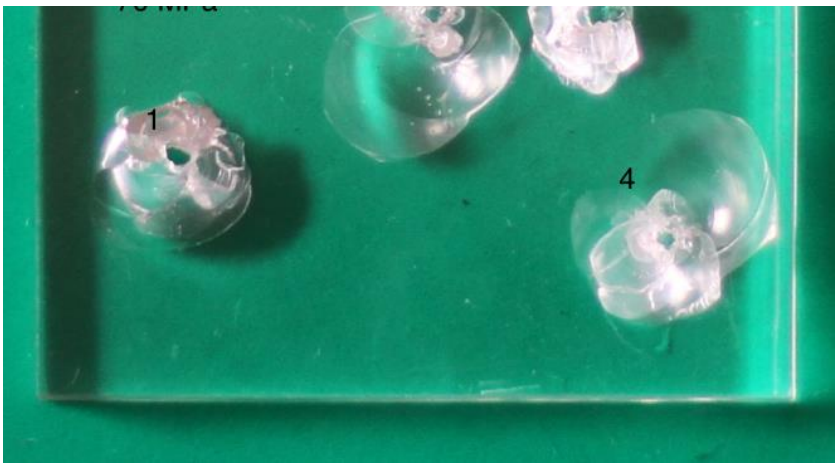

Figure 40: Drilling results, P45

Figure 41: Drilling results, P90

Drilling Depth

The UTM-setup at TU Delft provided a force input in order to create the desired water pressure. The water pressure was measured using a pressure sensor, located right before the device. The depth of the holes, seen in Fig.1-3, was measured using a dial gauge. These results can be seen in table 1-12.

P0	Iteration 1		
Force (kN)	Max Pressure (Mpa)	Ablation (y/n)	Hole depth (mm)
50	11.989	n	0
100	23.719	y	0.46
150	35.496	y	0.70
200	47.674	y	1.48
250	59.609	y	2.19
295	70.148	y	2.36

Table 5: Drilling pressure (MPa), drilling success, drilling depth (mm), P0, iteration 1

P0	Iteration 2		
Force (kN)	Max Pressure (Mpa)	Ablation (y/n)	Hole depth (mm)
50	11.771	n	0
100	23.516	y	0.39
150	35.738	y	0.92
200	47.631	y	1.47
250	59.516	y	2.12
295	70.215	y	2.67

Table 6: Drilling pressure (MPa), drilling success, drilling depth (mm), P0, iteration 2

P0	Iteration 3		
Force (kN)	Max Pressure (Mpa)	Ablation (y/n)	Hole depth (mm)
50	11.833	n	0
100	23.961	y	0.41
150	35.900	y	0.77
200	47.291	y	1.29
250	59.838	y	2.08
295	70.479	y	1.97

Table 7: Drilling pressure (MPa), drilling success, drilling depth (mm), P0, iteration 3

P0	Iteration 4		
Force (kN)	Max Pressure (Mpa)	Ablation (y/n)	Hole depth (mm)
50	11.840	n	0
100	24.116	y	0.43
150	36.124	y	0.77
200	47.996	y	1.22

250	59.230	y	1.98
295	70.346	y	2.08

Table 8: Drilling pressure (MPa), drilling success, drilling depth (mm), P0, iteration 4

P45	Iteration 1		
Force (kN)	Max Pressure (Mpa)	Ablation (y/n)	Hole depth (mm)
50	11.870	n	0
100	23.896	y	0.41
150	35.539	y	1.10
200	47.708	y	1.41
250	59.589	y	1.76
295	70.375	y	5

Table 9: Drilling pressure (MPa), drilling success, drilling depth (mm), P45, iteration 1

P45	Iteration 2		
Force (kN)	Max Pressure (Mpa)	Ablation (y/n)	Hole depth (mm)
50	11.894	n	0
100	23.778	y	0.43
150	35.592	y	1.08
200	47.467	y	1.42
250	59.154	y	2.20
295	70.313	y	2.52

Table 10: Drilling pressure (MPa), drilling success, drilling depth (mm), P45, iteration 2

P45	Iteration 3		
Force (kN)	Max Pressure (Mpa)	Ablation (y/n)	Hole depth (mm)
50	11.883	n	0
100	23.885	y	0.62
150	35.758	y	0.87
200	47.540	y	1.67
250	59.456	y	1.90
295	70.286	y	2.56

Table 11: Drilling pressure (MPa), drilling success, drilling depth (mm), P45, iteration 3

P45	Iteration 4		
Force (kN)	Max Pressure (Mpa)	Ablation (y/n)	Hole depth (mm)
50	11.917	n	0
100	23.753	y	0.67
150	35.521	y	0.97
200	47.524	y	1.53
250	59.159	y	1.80
295	70.491	y	2.38

Table 12: Drilling pressure (MPa), drilling success, drilling depth (mm), P45, iteration 4

P90	Iteration 1		
Force (kN)	Max Pressure (Mpa)	Ablation (y/n)	Hole depth (mm)
50	11.910	n	0
100	23.857	y	0.45
150	35.766	y	1.32
200	47.731	y	2.03
250	59.404	y	1.98
295	70.048	y	5

Table 13: Drilling pressure (MPa), drilling success, drilling depth (mm), P90, iteration 1

P90	Iteration 2		
Force (kN)	Max Pressure (Mpa)	Ablation (y/n)	Hole depth (mm)
50	11.919	n	0
100	23.757	y	0.56
150	35.719	y	1.10
200	47.454	y	1.81
250	59.547	y	3.67
295	70.165	y	2.25

Table 14: Drilling pressure (MPa), drilling success, drilling depth (mm), P90, iteration 2

P90	Iteration 3		
Force (kN)	Max Pressure (Mpa)	Ablation (y/n)	Hole depth (mm)
50	11.922	n	0
100	23.797	y	0.49
150	35.625	y	1.11
200	47.755	y	1.50
250	59.659	y	3.39
295	70.396	y	3.11

Table 25: Drilling pressure (MPa), drilling success, drilling depth (mm), P90, iteration 3

P90	Iteration 4		
Force (kN)	Max Pressure (Mpa)	Ablation (y/n)	Hole depth (mm)
50	11.939	n	0
100	23.736	y	0.45
150	35.650	y	1.23
200	47.413	y	1.29
250	59.508	y	1.93
295	70.096	y	5

Table 16: Drilling pressure (MPa), drilling success, drilling depth (mm), P90, iteration 4

Coherence

The jet coherence was recorded, using a camera, during jetting in free space. The still frames from these videos were captured and analysed using ImageJ software. By using the nozzle size as a frame of reference, the jet width was measured at the orifice (d1) and at the stand-off distance (l) the width was measured again (d2). These measurements were done for all three prototypes at all pressures where drilling success was recorded. The results are shown in tables 13-15.

P0	**100**	**150**	**200**	**250**	**295**
d1	1.241	1.283	1.287	1.278	1.266
d2	2.036	2.123	2.045	2.086	2.128
l	10.035	10.040	10.010	10.036	10.03

Table 16: Jet coherence P0: origin diameter (d1), end diameter (d2) and stand-off distance (l)

P45	**100**	**150**	**200**	**250**	**295**
d1	1.244	1.285	1.190	1.253	1.208
d2	2.002	2.165	2.545	2.214	2.216
l	10.005	10.028	10.034	10.013	10.008

Table 17: Jet coherence P45: origin diameter (d1), end diameter (d2) and stand-off distance (l)

P90	**100**	**150**	**200**	**250**	**295**
d1	1.282	1.250	1.216	1.211	1.243
d2	2.106	2.006	2.030	2.184	2.132
l	10.014	10.033	10.031	10.028	10.030

Table 18: Jet coherence P90: origin diameter (d1), end diameter (d2) and stand-off distance (l)

References

1. den Dunnen, S., et al., *Colliding jets provide depth control for water jetting in bone tissue.* Journal of the Mechanical Behavior of Biomedical Materials, 2017. **72**: p. 219-228.
2. den Dunnen, S., et al., *Pure waterjet drilling of articular bone: an in vitro feasibility study.* Strojniški vestnik-Journal of Mechanical Engineering, 2013. **59**(7-8): p. 425-432.
3. den Dunnen, S., et al., *Waterjet drilling in porcine bone: The effect of the nozzle diameter and bone architecture on the hole dimensions.* Journal of the mechanical behavior of biomedical materials, 2013. **27**: p. 84-93.
4. Den Dunnen, S. and G. Tuijthof, *The influence of water jet diameter and bone structural properties on the efficiency of pure water jet drilling in porcine bone.* Mechanical Sciences, 5 (2), 2014, 2014.
5. Erggelet, C., *Enhanced Marrow Stimulation Techniques for Cartilage Repair.* Operative Techniques in Orthopaedics, 2014. **24**(1): p. 2-13.
6. Haughom, B.D., et al., *Arthroscopic acetabular microfracture with the use of flexible drills: a technique guide.* Arthroscopy techniques, 2014. **3**(4): p. e459-e463.
7. Chen, H., et al., *Drilling and microfracture lead to different bone structure and necrosis during bone-marrow stimulation for cartilage repair.* Journal of Orthopaedic Research, 2009. **27**(11): p. 1432-1438.
8. Chillman, A., M. Hashish, and M. Ramulu, *Energy based modeling of ultra high-pressure waterjet surface preparation processes.* Journal of Pressure Vessel Technology, 2011. **133**(6): p. 061205.
9. Sudo, K., M. Sumida, and H. Hibara, *Experimental investigation on turbulent flow through a circular-sectioned 180 bend.* Experiments in Fluids, 2000. **28**(1): p. 51-57.
10. Kawamura, T., H. Takami, and K. Kuwahara, *Computation of high Reynolds number flow around a circular cylinder with surface roughness.* Fluid Dynamics Research, 1986. **1**(2): p. 145-162.
11. Mithoefer, K., et al., *Clinical efficacy of the microfracture technique for articular cartilage repair in the knee an evidence-based systematic analysis.* The American journal of sports medicine, 2009. **37**(10): p. 2053-2063.
12. Steadman, J.R., W.G. Rodkey, and J.J. Rodrigo, *Microfracture: surgical technique and rehabilitation to treat chondral defects.* Clinical orthopaedics and related research, 2001. **391**: p. S362-S369.
13. Gomoll, A.H., et al., *The subchondral bone in articular cartilage repair: current problems in the surgical management.* Knee Surgery, Sports Traumatology, Arthroscopy, 2010. **18**(4): p. 434-447.
14. Kandasamy, M., et al., *Integral force/moment waterjet model for cfd simulations.* Journal of Fluids Engineering, 2010. **132**(10): p. 101103.
15. Guha, A., R.M. Barron, and R. Balachandar, *Numerical simulation of high-speed turbulent water jets in air.* Journal of hydraulic research, 2010. **48**(1): p. 119-124.

16. Hultmark, M., et al., *Turbulent pipe flow at extreme Reynolds numbers.* Physical review letters, 2012. **108**(9): p. 094501.
17. ITO, H., *Flow in curved pipes.* JSME international journal: bulletin of the JSME, 1987. **30**(262): p. 543-552.
18. Eggers, J. and E. Villermaux, *Physics of liquid jets.* Reports on progress in physics, 2008. **71**(3): p. 036601.
19. Tikhomirov, R.A., et al., *High-pressure jetcutting.* Mechanical Engineering-CIME, 1992. **114**(6): p. 88-92.
20. Norušis, M.J., *SPSS 14.0 guide to data analysis*. 2006: Prentice Hall Upper Saddle River, NJ.
21. Geskin, E. and L. Tismeneskiy, *Mathematical modeling and experimental verification of stationary waterjet cleaning process.* Journal of manufacturing science and engineering, 1998. **120**: p. 571.
22. Yang, Y., et al., *Reaction thrust of submerged water jets.* Proceedings of the Institution of Mechanical Engineers, Part A: Journal of Power and Energy, 2007. **221**(4): p. 565-573.
23. Huang, G.-q., et al., *Reaction thrust of water jet for conical nozzles.* Journal of Shanghai University (English Edition), 2009. **13**: p. 305-310.
24. Ramsey, D.K. and P.F. Wretenberg, *Biomechanics of the knee: methodological considerations in the in vivo kinematic analysis of the tibiofemoral and patellofemoral joint.* Clinical Biomechanics, 1999. **14**(9): p. 595-611.
25. Dickinson, W., R. Anderson, and R. Dickinson, *The ultrashort-radius radial system.* SPE Drilling engineering, 1989. **4**(03): p. 247-254.
26. Glozman, D., et al., *A self-propelled inflatable earthworm-like endoscope actuated by single supply line.* IEEE Transactions on Biomedical Engineering, 2010. **57**(6): p. 1264-1272.
27. Masson, J.B., S.A. Bugami, and J.G. Webb, *Endovascular balloon occlusion for catheter-induced large artery perforation in the catheterization laboratory.* Catheterization and Cardiovascular Interventions, 2009. **73**(4): p. 514-518.
28. Wabeke, D.T., G. and Dankelman, J. , *Water-Jet Stability Through Flexible Tubing for Microsurgery*. 2016.
29. Rinaldi, S. and M. Païdoussis, *Dynamics of a cantilevered pipe discharging fluid, fitted with a stabilizing end-piece.* Journal of Fluids and Structures, 2010. **26**(3): p. 517-525.